

Relationship between the Contrast of Coronal Holes and Parameters of the Solar Wind Streams

V. N. Obridko¹, B. D. Shelting¹, I. M. Livshits¹, and A. B. Askerov²

¹*Pushkov Institute of Terrestrial Magnetism, Ionosphere, and Radio Wave Propagation,
Russian Academy of Sciences, Troitsk, Moscow oblast, 142190 Russia*

²*Shemakha Astrophysical Observatory, National Academy of Sciences of Azerbaijan Republic,
Yu. Mamedaliev Settlement, Azerbaijan*

Received March 15, 2009; in final form, April 7, 2009

Abstract—It is shown that the contrast of coronal holes (CH) determines the speed of the solar wind streams to the same extent as their area does. We analyzed more than 400 images obtained in the $\lambda 284 \text{ \AA}$ channel. The time interval under examination covers about 1500 days in the declining phase of cycle 23 (from 2002 to 2006). We considered all coronal holes recorded during that interval in the absence of coronal mass ejections (CME). Comparison was also made with some other parameters of the solar wind (e.g., density, temperature, and magnetic field). A fairly high correlation (0.70–0.89) was obtained with the velocity, especially during the periods of moderate activity, which makes this method useful for everyday forecast. The ratio of CH brightness to the mean brightness of the disk in the $\lambda 284 \text{ \AA}$ channel is about 25%.

PACS numbers: 96.50.Ci, 96.60.pc, 96.60.Vg

DOI: 10.1134/S1063772909110109

1. INTRODUCTION

Soon after coronal holes (CH) had been discovered in the Sun, it became clear that they were associated with high-speed streams (HSS) of the solar wind (SW). Nolte et al. [1] established a close relationship between the speed of the solar wind streams from a coronal hole and the area of the latter. Later on, the relationship between CH and HSS was demonstrated by various authors [2–6]. Coronal holes usually appear as dark features on the solar disk in the X-ray, extreme ultraviolet, and radio wavelength ranges [6, 7].

There are some physical reasons to believe that the brightness (contrast) of CH must correlate with some characteristics of the associated HSS, first of all, with their velocity. This suggestion was made about ten years ago in [8, 9], but it has not been verified ever since. Another relationship, i.e., the correlation between the velocity and CH area, was verified more than once [10–13]. In particular, Robbins et al. [11] have shown that the correlation between the solar wind velocity and CH area decreases in the epochs of high solar activity. This should be expected, because coronal mass ejections (CME) not related directly to coronal holes produce sudden bursts of speed, which upset the correlation with CH area. Besides, the role of closed field lines responsible for the particularly slow streams increases in the periods of high solar

activity. Vrsnak et al. [12, 13] studied the relationship between the solar wind velocity and CH area in a relatively quiet period—from January to May, 2005, and obtained a reasonably high correlation coefficient (0.62) at a transport time of 4 days.

Many authors analyzed the relationship between the CH magnetic field and solar wind velocity. Thus, Belov et al. [14] obtained quite a high correlation between the magnetic field parameters in the Sun and the speed of the solar wind. The routine forecast of the solar wind speed based on potential extrapolation of the observed photospheric field is issued by several prognostic centers.

Using one of these models—a modified flux-transport model [15, 16],—Arge and Pizzo [17] studied a 3-year period centered about the solar minimum of May 1996 and obtained the correlation coefficient equal to ~ 0.4 . Later on, the model was updated significantly. Now, it takes into account the distance to the nearest CH by the same method of potential approximation [18, 19]. The results of calculations are available on the Internet site <http://www.swpc.noaa.gov/ws/>.

However, since the CH brightness (contrast) depends on the divergence of the field lines, which also determines the HSS velocity, the correlation between these quantities is physically justified and can be used as a reasonable parameter for the geophysical

forecast. It is clear today that coronal holes are the areas of open magnetic field, where coronal plasma flows out efficiently into the solar wind. As a result, the corona in these regions gets empty of plasma, and its brightness decreases. Different brightness of coronal holes and the ambient corona is a result of the difference in the heating and energy loss mechanisms [20–25]. While the regular corona loses energy through heat conduction, the loss in CH is mainly due to the outflow of the solar wind [26]. Thus, the very fact of darkening in the coronal holes is, undoubtedly, associated with the escape high-speed streams. The same conclusion was drawn in [27, 28].

Many uncertainties that will be discussed below have prevented us so far from using directly our hypothesis of correlation between the CH brightness and solar wind velocity proposed earlier in [8, 9]. The CH brightness (“darkness”) is used as a subsidiary qualitative prognostic factor at the Center of Forecasts of IZMIRAN. However, it is difficult to verify this correlation and obtain quantitative characteristics.

Lately, Luo et al. [29] calculated the solar wind velocity at the Earth from CH brightness in the channel $\lambda 284 \text{ \AA}$ and obtained quite a high correlation for a relatively short time interval from November 21 to December 26, 2003. It should be noted, however, that the prognostic index they used was not the CH brightness per se but the inverse brightness in each pixel averaged over a particular circle at the center of the Sun. This value may differ significantly from the mean brightness. It is difficult to interpret physically, since in all heating and energy transport mechanisms, we are dealing with the brightness rather than its inverse value. Besides, the inverse brightness averaged over a particular circle may involve nonstationary processes, such as flares and coronal mass ejections, and thus, may corrupt the index obtained. On small time scales, however, all indices (area, brightness, and inverse brightness) will give equally good results, because the CH parameters change relatively slow.

In view of the aforesaid, we decided to follow the direct path, i.e., to use the pixel brightness over a large time interval and to investigate the potential sources of uncertainty associated both with the physical analysis of CH brightness and with its prognostic application. The checking calculations were performed for several periods, including those analyzed in [12, 13, 29].

2. DATA AND METHODS

The work involves certain difficulties associated with poor definition of many characteristics and even terms. Unfortunately, no quantitative criteria are

available to reliably single out coronal holes from observations [30].

In particular, we do not know for certain what is the boundary of a coronal hole, what wavelengths it should be studied at, how it can be discriminated from the filament-type features, how the contrast is determined, what is the undisturbed region, and how the potential degradation of receivers can be allowed for. We do not know whether the polar and equatorial holes must be analyzed separately.

Figure 1 illustrates the situation on the disk as observed on November 28, 2002 in the channel $\lambda 284 \text{ \AA}$.

A complex feature of CH type was observed on the disk on that day. Its boundaries are extremely difficult to identify, and its contours are multiconnected. Since the inner structure of the hole is highly inhomogeneous, it is not clear whether we must consider its minimum brightness, mean brightness, or full integral deficit of brightness (or, to speak figuratively, “the maximum depth,” “the mean depth,” or “the volume of the canyon”). Comparison with the solar wind parameters involves additional difficulties associated with isolating the CH effect and eliminating the other processes, first of all, coronal mass ejections. Therefore, the solution of the problem is divided into several stages.

The contrast is calculated by the method commonly used in the photometry of spectral lines or sunspots. One needs for calculation the measurements of the background or fogging (in our case, outside the disk), the CH proper brightness, and variation in the undisturbed region (equivalent of the continuum in the spectral photometry). Even so, it is not clear whether the deficit should be found against the mean brightness of the disk, which contains many isolated, very bright features, or against the CH immediate environment. Note also that though coronal holes are sharply pronounced on the images, their real contrast is not too large. E.g., it is much lower than in sunspots.

There is another problem to be solved. We can compare the brightness of coronal holes with the solar wind velocity directly on the days when the former pass over the disk. Alternatively, we can simulate the everyday forecast by calculating the prognostic indices for each day whether or not any CH are observed. In doing so, we must, naturally, exclude the days when coronal mass ejections occur, since these events are controlled by absolutely different physical mechanisms.

Correlation with the solar wind parameters involves one more source of uncertainty, i.e., the transport time. Note that the optimal transport time may not be the same for different solar wind parameters.

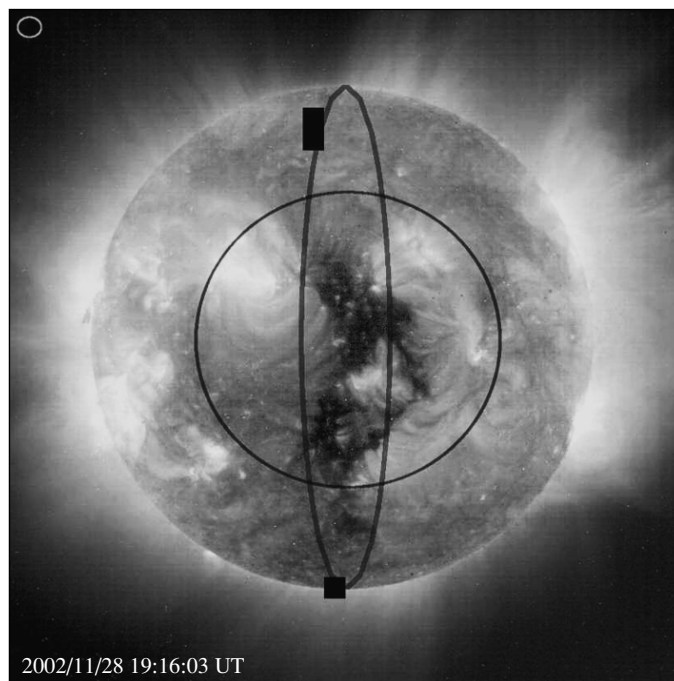


Fig. 1. Coronal hole observed in the channel $\lambda 284 \text{ \AA}$ on November 28, 2002. The circle in the upper left angle marks the site where background measurements were taken (see Subsection 2.2). The boundaries of the spherical sector and circle of radius $0.6 R_{\odot}$ are shown.

2.1. Preview of Data

Coronal holes are observed as dark features on the SOHO/EIT and STEREO/EUVI X-ray and UV images [6, 7].

In the epoch of solar maximum, the polar holes are absent, but there are many equatorial holes, which are more convenient to establish the relationship with the increase of the solar wind velocity. On the other hand, this is the period when undisturbed regions are rare, and there is a high probability that the acceleration is rather associated with CME than CH.

In the epoch of minimum, on the contrary, the equatorial holes are absent, while the polar holes are present at all times. In this period, it is easier to determine the undisturbed background. One can simply use daily observations and sum up the daily areas of the regions whose brightness is below a certain limit.

We began our study with 1999. The database we examined comprises SOHO observations at the wavelengths of 171 \AA ($T \sim 1.3 \times 10^4 \text{ K}$), 195 \AA ($T \sim 1.6 \times 10^6 \text{ K}$), 284 \AA ($T \sim 2.0 \times 10^6 \text{ K}$), 304 \AA ($T \sim 8.0 \times 10^4 \text{ K}$), YOHKOH X-ray data, sketches of CH as observed in the line 10830 \AA from “Solar-Geophysical Data,” open magnetic fields calculated by our own program from the Stanford data, and the summary file of observations of the solar wind speed at the Earth. Four coronal holes whose passages

through the central meridian could be associated more or less reliably with the increases in SW velocity were selected.

The line 284 \AA proved to suit best for our study, in which context it should be noted that:

- The contrast is estimated by the method commonly used in the photometry of spectral lines or sunspots. One needs for calculation the measurements of the background or fogging. Having examined the data for 2005, we found out that the background did not virtually change during a year and could be determined with an error less than 0.2%.
- The brightness of undisturbed region is extremely uncertain and, therefore, is difficult to use.
- We have taken as a conventional boundary of CH or (the same thing in our case) the brightness of its undisturbed environment 1.03 of the fog value. As shown by preliminary estimates, this does not affect much the result, because the brightness at the boundary does not change fast. The indices obtained alter a little if we use the values of 1.035 and 1.04 of the background brightness, but the correlation

with the solar wind parameters remains virtually unchanged.

- The calculations for each day are performed for the entire disk, for a spherical sector of $\pm 13.3^\circ$ from the central meridian in the heliographic coordinates, and for a circle of radius equal to 0.6 solar radii.
- In this study, we do not introduce correction for the projection, and all areas are calculated as the number of pixels.
- The defects like those seen in Fig. 1 are dealt with by taking the mean disk value for the pixels involved. This does not virtually affect the mean contrast.

2.2. Initial Data and Indices Obtained

We have used the SOHO data in the fits—format 1024×1024 from the site http://sohowww.nascom.nasa.gov/cgi-bin/summary_query_form. The CH list was downloaded from the site http://www.solen.info/solar/coronal_holes.html (“Coronal hole history (since late October 2002)”). Comparison was made with the daily mean values of velocity V , magnetic field B , density n , and temperature T at the transport times of 2, 3, and 4 days. These data were taken from the site <http://omniweb.gsfc.nasa.gov/>.

The following parameters were calculated for each day:

General characteristics

fon—the minimum image brightness beyond the solar disk,

S1—the total pixel brightness over the disk,

d1—the total number of pixels on the disk,

ss1—the mean brightness of a pixel on the disk ($ss1 = S1/d1$).

Central characteristics calculated by two methods:

(a) inside a spherical sector of $\pm 13.3^\circ$ from the central meridian

and (b) inside a circle of radius $0.6R_\odot$

S2—the total pixel brightness,

d2—the number of pixels,

ss2—the mean brightness ($ss2 = S2/d2$).

CH characteristics also calculated by two methods:

(a) inside a spherical sector of $\pm 13.3^\circ$ from the central meridian

and (b) inside a circle of radius $0.6R_\odot$

sk—the total brightness of the pixels that satisfy the condition “brightness below $f_i * fon$.” The value f_i determining, the CH brightness boundary was taken equal to 1.03,

dkd—the number of pixels that satisfy the condition “brightness below $f_i * fon$,”

skd—the mean brightness of the pixels that satisfy the condition “brightness below $f_i * fon$,”

ou—the minimum brightness among the points pertinent to CH.

Indices

cn1 = $(ss - skd) * dkd$ —the volume of canyon provided that the undisturbed level equals the mean disk brightness,

ou—the minimum brightness among the points pertinent to CH,

A = $dkd/d2$ —the relative CH area inside the central sector. Corresponds to the index used in [12, 13],

cn2 = $(ss2 - skd) * dkd$ —the volume of canyon provided that the undisturbed level equals the mean brightness in the central sector,

cn3 = $(1.03 * fon - skd) * dkd$ —the volume of canyon provided that the undisturbed level equals $1.03 * fon$,

dcn = $1.03 * fon - skd$ —the mean depth of canyon provided that the undisturbed level equals $1.03 * fon$,

dmax = $1.03 * fon - ou$ —the maximum depth of canyon provided that the undisturbed level equals $1.03 * fon$.

Some of the parameters (indices) listed above are illustrated on one-dimensional section across the disk center for November 28, 2002 (Fig. 2).

The parameters R_\odot , X_0 , and Y_0 determining the radius and coordinates of the disk center for this day in pixels were taken from the file header. This ensured that the eccentricity of the Earth orbit was taken into account. The size of a pixel in seconds and the exposure including the shutter time were also registered, but no correction was made for these values, because they changed very little ($< 0.5\%$).

As said above, the contrast is rather difficult to estimate, since it is not clear what it must be compared to. If the contrast is determined against the fon value as it is done below in Fig. 3, we obtain very small values in the range of 0.003–0.010. However, the fon value on these images is very high, reaching 830–840 counting units per pixel. The excess of the disk mean brightness over the fon value without regard for the

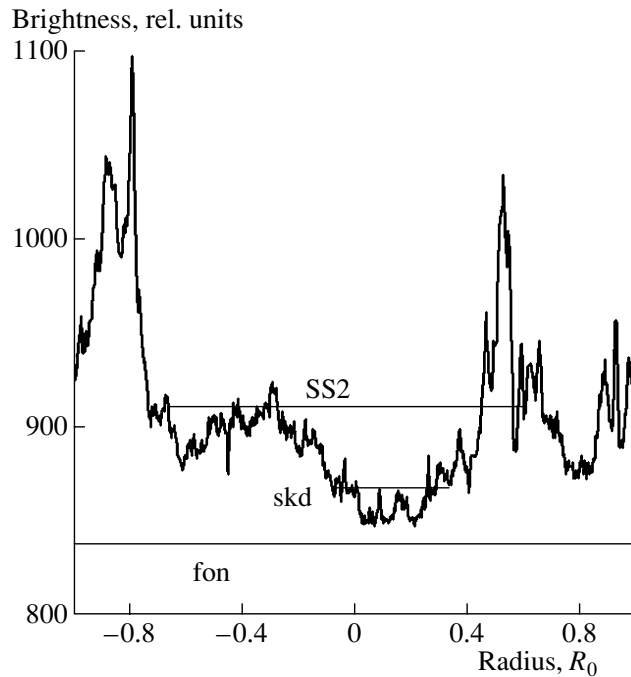


Fig. 2. One-dimensional central section of the disk brightness on November 28, 2002. Some of the indices used are shown.

projection is 70 units in 2002 and decreases gradually down to 50 units in 2007. If we assume the fon value to be the reference level and relate dcn values to the mean disk excess over this level, we obtain the relative mean brightness of CH equal to $\sim 25\%$.

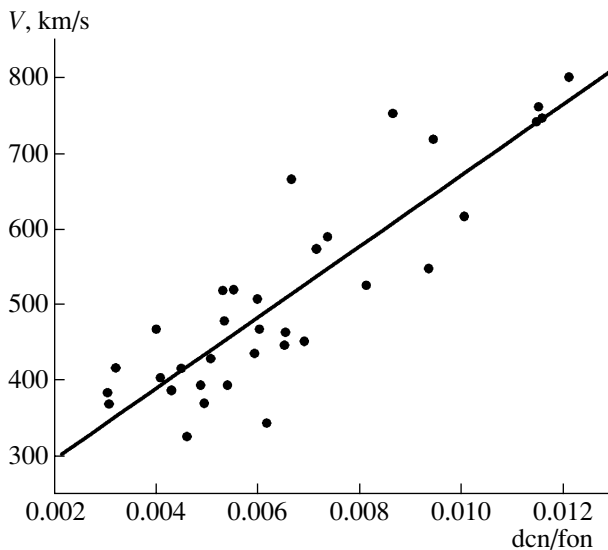


Fig. 3. Correlation between the mean darkening dcn and SW speed in the period from November 21 to December 26, 2003.

3. COMPARISON OF CH CONTRAST AND SOLAR WIND PARAMETERS

We selected for the analysis 138 coronal holes for the period 2002–2006 from the file “Coronal hole history (since late October 2002),” i.e., all CH associated with SW acceleration at the Earth in the absence of coronal mass ejections. Table 1 provides the correlation between SW parameters and CH brightness. The comparison of five CH indices with four SW parameters leads us to the following conclusions:

1. The index **dcn**, i.e., the mean deficit, is most convenient for calculating the SW speed at a transport time of 4 days.

2. None of the indices under examination is too good for the field and density calculations. We can only note that all of them display anti-correlation with density on the fourth day, i.e., at the time of maximum velocity.

3. The positive correlation of dcn with temperature is rather high at a shift of 2–3 days.

4. Calculation of the magnetic field from CH brightness does not offer much advantage. The traditional method of calculating the source surface field from magnetographic data seems more promising. This method was used, in particular, in [14].

To check the CH effect and take into account the distance from the central meridian, we calculated all indices under consideration inside a circle of radius

Table 1. Correlation between CH indices in the central sector and SW parameters

Index	$\delta t = 2$ days				$\delta t = 3$ days				$\delta t = 4$ days			
	<i>B</i>	<i>V</i>	<i>n</i>	<i>T</i>	<i>B</i>	<i>V</i>	<i>n</i>	<i>T</i>	<i>B</i>	<i>V</i>	<i>n</i>	<i>T</i>
	Correlation coefficient											
A	0.28	0.35	0.05	0.40	0.00	0.48	-0.20	0.37	0.25	0.48	-0.33	0.22
cn2	0.16	0.33	-0.05	0.33	0.21	0.30	-0.14	0.22	0.12	0.26	-0.17	0.13
cn3	0.22	0.41	-0.05	0.42	0.00	0.49	-0.22	0.35	0.18	0.47	-0.29	0.22
dcn	0.36	0.49	-0.06	0.50	0.24	0.62	-0.29	0.51	0.00	0.63	-0.30	0.37
dmax	0.24	0.44	-0.10	0.40	0.25	0.47	-0.23	0.39	0.05	0.51	-0.28	0.36

Table 2. Correlation between CH indices in the central circle and CH parameters

Index	$\delta t = 2$ days				$\delta t = 3$ days				$\delta t = 4$ days			
	<i>B</i>	<i>V</i>	<i>n</i>	<i>T</i>	<i>B</i>	<i>V</i>	<i>n</i>	<i>T</i>	<i>B</i>	<i>V</i>	<i>n</i>	<i>T</i>
	Correlation coefficient											
A	0.29	0.43	0.00	0.52	0.00	0.54	-0.23	0.41	0.26	0.54	-0.36	0.30
cn2	0.26	0.25	-0.12	0.33	0.20	0.28	-0.11	0.24	0.10	0.30	-0.24	0.20
cn3	0.32	0.59	-0.13	0.63	0.00	0.65	-0.32	0.48	0.18	0.65	-0.39	0.40
dcn	0.36	0.62	-0.16	0.60	0.24	0.67	-0.33	0.54	0.00	0.68	-0.37	0.42
dmax	0.23	0.53	-0.18	0.45	0.23	0.51	-0.26	0.40	0.00	0.53	-0.35	0.39

$0.6R_{\odot}$ for the 138 CH mentioned above. The calculation results are tabulated in Table 2. The comparison shows that correlation between the indices under examination and SW velocity with allowance for the transport time $\delta t = 3 - 4$ days somewhat increases from Table 1 to Table 2. This is, probably, because the polar holes were excluded from consideration. The increase, however, exceeds only slightly the correlation coefficient error equal to 0.04. Nevertheless, the second method is preferable when comparing CH observations on the disk with SW velocity.

4. CALCULATION OF SW PARAMETERS IN EVERYDAY FORECASTING PRACTICE

At first sight, the problem of estimating SW parameters for the everyday forecast could be solved by comparing them directly with the CH brightness deficit as described in the previous Section. However, there are two factors that keep us from doing so:

1. The database the everyday forecast is dealing with involves the days when no CH are observed on the disk. This expands the general dynamic range of the data.

2. Occasionally, coronal holes are accompanied by CME events, which change the velocity range dramatically. As seen below, the correlation between the brightness and SW velocity on such days is violated completely.

First of all, we analyzed the interval from January 20 to June 5, 2005, i.e., the days of the year number 20–125. The days number 70–90, for which the $\lambda 284 \text{ \AA}$ data are unavailable, were omitted. In the interval under consideration, the halo CMEs were absent. So, we can suggest that the solar wind was undisturbed, and its variations were controlled totally by coronal holes. The first part of this interval coincides with the period analyzed in [12, 13].

Tables 3 and 4 provide the correlation of the calculated indices with *B*, *V*, *n*, *T*, and *A_p* at different transport times in everyday forecast. As above, the calculations were made for the spherical sector of $\pm 13.3^\circ$ from the central meridian (Table 3) and for the circle of radius $0.6R_{\odot}$ (Table 4).

Here, too, the dcn parameter is obviously the best. The highest correlation with *V* is obtained on the fourth day, with *B* on the second day, with *n* on the first day, and with *T* on the third day.

Table 3. Correlation between the daily deficit of brightness in the central sector and solar wind parameters

Index	$\delta t = 2$ days					$\delta t = 3$ days					$\delta t = 4$ days				
	<i>B</i>	<i>V</i>	<i>n</i>	<i>T</i>	<i>A_p</i>	<i>B</i>	<i>V</i>	<i>n</i>	<i>T</i>	<i>A_p</i>	<i>B</i>	<i>V</i>	<i>n</i>	<i>T</i>	<i>A_p</i>
	Correlation coefficient														
A	0.29	0.16	0.27	0.30	0.28	0.25	0.49	0.07	0.46	0.31	0.04	0.67	-0.19	0.51	0.32
cn2	0.48	0.04	0.27	0.22	0.16	0.31	0.18	0.04	0.35	0.17	0.14	0.26	-0.13	0.24	0.13
cn3	0.37	0.04	0.33	0.31	0.33	0.32	0.52	0.07	0.53	0.39	0.05	0.71	-0.24	0.052	0.33
dcn	0.59	0.05	0.51	0.22	0.0	0.53	0.47	0.14	0.63	0.54	0.32	0.74	-0.21	0.55	0.37
dmax	0.47	0.0	0.41	0.17	0.0	0.46	0.44	0.11	0.54	0.40	0.24	0.66	-0.21	0.54	0.31

Table 4. Correlation between the daily deficit of brightness in the central circle and solar wind parameters

Index	$\delta t = 2$ days				$\delta t = 3$ days				$\delta t = 4$ days			
	<i>B</i>	<i>V</i>	<i>n</i>	<i>T</i>	<i>B</i>	<i>V</i>	<i>n</i>	<i>T</i>	<i>B</i>	<i>V</i>	<i>n</i>	<i>T</i>
	Correlation coefficient											
A	0.27	0.17	0.26	0.29	0.23	0.47	0.00	0.45	0.00	0.62	-0.20	0.47
cn2	0.39	0.12	0.18	0.36	0.24	0.24	-0.08	0.33	0.06	0.22	-0.26	0.24
cn3	0.36	0.14	0.32	0.31	0.31	0.50	0.03	0.50	0.06	0.68	-0.24	0.50
dcn	0.59	0.03	0.49	0.27	0.55	0.48	0.10	0.60	0.26	0.68	-0.30	0.49
dmax	0.45	0.10	0.36	28	0.37	0.45	0.29	0.51	0.04	0.63	-0.28	0.52

There are some differences between Tables 1–2 and Tables 3–4:

1. When analyzing the relationship between coronal holes and solar wind parameters, we obtained somewhat higher correlation when using the data inside the circle of radius $0.6 R_{\odot}$, i.e., in the equatorial zone corresponding to the distance of ± 3 days ($\pm 37^{\circ}$) from the central meridian (the polar zone was excluded). In the everyday forecast, on the contrary, the correlation is higher for the spherical sector of $\pm 13.3^{\circ}$ from the central meridian.

2. Whereas in Tables 1–2, we see negative correlation between the CH brightness and SW density n at small transport times, in Tables 3–4, it is only established at a shift of 4 days.

3. The correlation turned out to be fairly high with T at $\delta t = 3$.

4. As for correlation with the geomagnetic activity index A_p , it is poor in both cases. To calculate this index correctly, we, obviously, have to take into account solar magnetic data [14].

Finally, we have chosen the period from November 21 to December 26, 2003, when no coronal mass ejections were recorded. This short period was also

used in the work [29]. In both works, the mean brightness and velocity correlate at a time shift of 4 days with the same coefficient equal to 0.88.

Figure 3 is the diagram representing the relationship between the mean deficit dcn and solar wind velocity in the period under discussion. The abscissa on the diagram is dcn/ion; however, this does not affect the correlation over such a short interval. Here the correlation equals 0.89 and coincides with that obtained on this time interval by Luo et al. [29].

The measured and calculated velocities for this time interval are juxtaposed in Fig. 4.

Thus, the method of calculating the velocity of quiet solar wind from the deficit of brightness in coronal holes is justified in the periods when coronal mass ejections are absent.

There is an important trait to emphasize. All twenty increases of velocity above 500 km/s recorded during the period under discussion are adequately described by our calculated curves. The mean difference between the calculated and measured values is less than 50 km/s.

It should be noted, however, that coronal mass ejections result in unpredictable velocity bursts,

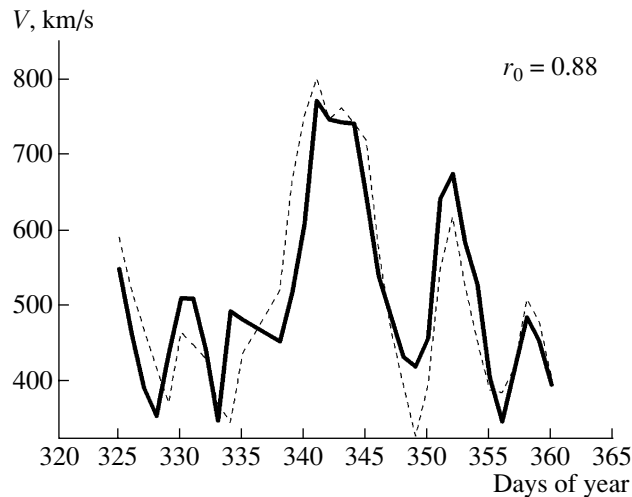


Fig. 4. Measured (dashed curve) and calculated (solid curve) velocities for the period from November 21 to December 26, 2003.

which, naturally, decrease the correlation. This was the case in the mid 2005 when the comparison of the calculated and measured velocities revealed six unpredicted increases of velocity. All of them, however, coincided in time with the halo CMEs observed in the Sun. At the end of the year, when coronal mass ejections were absent, the agreement between the measured and calculated velocities was restored.

5. CONCLUSIONS

Thus, the hypothesis of direct correlation between the CH contrast and velocity of the associated solar-wind streams was corroborated for all days in 2005 (270) for which $\lambda 284 \text{ \AA}$ observations are available, for 35 days in 2003, and for 138 separate CH observed from 2002 to 2006; i.e., the total of 443 correlations were considered. The analysis covered the time interval more than 1500 days in the declining phase of cycle 23. We analyzed all CH observed in the period under discussion in the absence of CME and obtained the correlation coefficients equal to 0.70 (sometimes reaching 0.88) at the transport time of four days. All velocity bursts above 500 km/s were successfully predicted. The mean difference between the measured and calculated velocities was less than 50 km/s. Significant correlations were also revealed with the other solar wind parameters, in particular, density and temperature, at a shift of 2–4 days.

The mean CH contrast in the time interval under consideration was 10–12% and the maximum, 33–40%. The contrast was observed to decrease as the minimum of cycle 23 was approached, while the mean area did not change.

It is shown that the indices discussed above can be used for everyday forecast. The advantage of this approach is the absence of theoretical assumptions. The correlation is only established between the directly measured parameters, and the correlation coefficients obtained are higher than in other methods.

Moreover, the correlation revealed is, in fact, an independent experimental evidence of the validity of our main concepts of the structure and heating of coronal holes.

We are grateful to the SOHO team for the data we downloaded from the SOHO Internet site http://sohowww.nascom.nasa.gov/cgi-bin/summary_query_form and to the authors of the sites http://www.solen.info/solar/coronal_holes.html (“Coronal hole history (since late October 2002)”) and <http://omniweb.gsfc.nasa.gov/>. We also thank A.V. Belov and I.M. Chertok for useful discussions. The work was supported by the Russian Foundation for Basic Research (project no. 08-02-00070).

REFERENCES

1. J. T. Nolte, A. S. Krieger, A. F. Timothy, et al., *Solar Phys.* **46**, 303 (1976).
2. J. T. Gosling and V. J. Pizzo, *Space Sci. Rev.* **89**, 21 (1999).
3. J. Zhang, J. Woch, S. K. Solanki, and R. von Steiger, *Geophys. Res. Lett.* **29**, 1236 (2002).
4. J. Zhang, J. Woch, S. K. Solanki, et al., *J. Geophys. Res.* **108**, 1144 (2003).
5. D. J. McComas and H. A. Elliot, *Geophys. Res. Lett.* **29**, 1314 (2002).
6. B. J. I. Bromage, P. K. Browning, and J. R. Clegg, *Space Sci. Rev.* **97**, 13 (2001).

7. S. W. Kahler and H. S. Hudson, *Astrophys. J.* **574**, 467 (2002).
8. V. N. Obridko, in *Advances in Solar Connection with Transient Interplanetary Phenomena, Proc. of the 3rd SOLTIP Symp., Beijing, China, Oct. 14–18, 1996*, Ed. by X. Feng, F. Wei, and M. Dryer (International Academic Publishers, Beijing, 1998), p. 41.
9. V. N. Obridko, V. V. Fomichev, A. F. Kharshiladze, et al., *Astron. Astrophys. Trans.* **18**, 819 (2000).
10. I. S. Veselovskii, I. G. Persiantsev, A. Yu. Rusanov, and Yu. S. Shugař, *Astron. Vestn.* **40**, 427 (2006) [*Solar Syst. Res.* **40**, 427 (2006)].
11. S. Robbins, C. J. Henney, and J. W. Harvey, *Solar Phys.* **233**, 265 (2006).
12. B. Vrsnak, M. Temmer, and A. M. Veronig, *Solar Phys.* **240**, 315 (2007).
13. B. Vrsnak, M. Temmer, and A. M. Veronig, *Solar Phys.* **240**, 331 (2007).
14. A. V. Belov, V. N. Obridko, and B. D. Shelting, *Geomagn. Aeron.* **46**, 430 (2006).
15. Y.-M. Wang and N. R. Sheeley, Jr., *Astrophys. J.* **355**, 726 (1990).
16. Y.-M. Wang and N. R. Sheeley, Jr., *Astrophys. J.* **392**, 310 (1992).
17. C. N. Arge and V. J. Pizzo, *J. Geophys. Res.* **105**, 10465 (2000).
18. C. N. Arge, D. Odstrcil, V. J. Pizzo, and L. R. Mayer, in *Solar Wind Ten: Proc. Tenth International Solar Wind Conference*, Ed. by M. Velli, R. Bruno, F. Malara, and B. Bucci (AIP Conf. Proc., New York, 2003), **679**, 190 (2003).
19. C. N. Arge, J. G. Luhmann, D. Odstrcil, et al., *J. Atmos. Sol. Terr. Phys.* **66**, 1295 (2004).
20. G. W. Cushman and W. A. Rense, *Astrophys. J. Lett.* **207**, L61 (1976).
21. G. J. Rottman, F. Q. Orrall, and J. A. Klimchuk, *Astrophys. J.* **260**, 326 (1982).
22. F. Q. Orrall, G. J. Rottman, and J. A. Klimchuk, *Astrophys. J. Lett.* **266**, L65 (1983).
23. S. R. Cranmer, “Coronal Holes,” in *Encyclopedia of Astronomy and Astrophysics*, Ed. by P. Murdin (Inst. of Phys., Bristol, 2001), article 1999.
24. S. R. Cranmer, *COSPAR Coll. Ser.* **13**, 3 (2002).
25. S. R. Cranmer, *Space Sci. Rev.* **101**, 229 (2002).
26. G. L. Withbroe and R. W. Noyes, in *Annual Review of Astronomy and Astrophysics* (Annual Reviews, Inc., Palo Alto, Calif., 1977), Vol. 15, p. 363.
27. O. G. Badalyan and V. N. Obridko, *Astron. Zh.* **81**, 746 (2004) [*Astron. Rep.* **48**, 678 (2004)].
28. O. G. Badalyan and V. N. Obridko, *Solar Phys.* **238**, 271 (2007), DOI 10.1007/s11207-006-0214-2.
29. B. Luo, Q. Zhong, S. Liu, and J. Gong, *Solar Phys.* **250**, 159 (2008).
30. X. P. Zhao, J. T. Hoeksema, and P. H. Scherrer, *J. Geophys. Res.* **104**, 9735 (1999).

Translated by the authors